IL-37/IL-1R8 blocks keratinocyte acantholysis via suppressing ADAM17/EGFR

FENGXIA HU[1,2*], WENJING CHEN[1*], QIAN WANG[1], XIAOYU ZHANG[1], FUYANG XIAO[1], JINYING ZHANG[3] and JUNQIN LIANG[1,2,4]

[1]Department of Allergy, People's Hospital of Xinjiang Uygur Autonomous Region, Urumqi, Xinjiang Uygur Autonomous Region 830001, P.R. China; [2]Xinjiang Key Laboratory of Dermatology Research, Urumqi, Xinjiang Uygur Autonomous Region 830001, P.R. China; [3]Chinese and Western Medicine Collaborative Diagnosis and Treatment Medical Center, People's Hospital of Xinjiang Uygur Autonomous Region, Urumqi, Xinjiang Uygur Autonomous Region 830001, P.R. China; [4]Treatment Center of Biomedicine, People's Hospital of Xinjiang Uygur Autonomous Region, Urumqi, Xinjiang Uygur Autonomous Region 830001, P.R. China

Received September 26, 2025; Accepted January 28, 2026

DOI: 10.3892/ijmm.2026.5793

Abstract. Pemphigus vulgaris (PV) is a life-threatening autoimmune blistering disease characterized by acantholysis (the loss of cell-cell adhesion of keratinocytes) and the formation of non-healing suprabasal intraepidermal blisters. The progression of keratinocyte acantholysis in PV is complex. Interleukin-37 (IL-37), which functions through receptor binding, exerts a protective role in PV. However, the specific receptor mediating the effect of IL-37 in PV and the underlying mechanisms remain unclear. The present study found elevated levels of IL-37, a natural suppressor of innate inflammatory and immune responses, in patients with PV. IL-37 treatment directly suppressed both acantholysis and apoptosis in keratinocytes. Mechanistic investigations using co-immunoprecipitation revealed that IL-37 binds to interleukin-1 receptor 8 (IL-1R8). Knockdown of IL-1R8 (or IL-18Rα) abolished the inhibitory effects of IL-37 on acantholysis and apoptosis. Furthermore, the IL-37/IL-1R8 complex suppressed epidermal growth factor receptor (EGFR) signaling, and reduced the expression of TNF-alpha-converting enzyme (ADAM17). Activation of EGFR using specific agonists reversed the IL-37-mediated reduction in acantholysis and apoptosis in HaCaT cells. In conclusion, IL-37 treatment markedly attenuated keratinocyte dissociation and apoptosis in PV through the IL-1R8/ADAM17/EGFR pathway. These findings provide novel mechanistic insights into the immunoregulatory functions of IL-37.

Correspondence to: Professor Jinying Zhang, Chinese and Western Medicine Collaborative Diagnosis and Treatment Medical Center, People's Hospital of Xinjiang Uygur Autonomous Region, 91 Tianchi Road, Tianshan, Urumqi, Xinjiang Uygur Autonomous Region 830001, P.R. China
E-mail: 1461906789@qq.com

Professor Junqin Liang, Department of Allergy, People's Hospital of Xinjiang Uygur Autonomous Region, 91 Tianchi Road, Tianshan, Urumqi, Xinjiang Uygur Autonomous Region 830001, P.R. China
E-mail: drliangjq@163.com

*Contributed equally

Key words: pemphigus vulgaris, interleukin-37, acantholysis, TNF-alpha-converting enzyme, epidermal growth factor receptor

Introduction

Pemphigus vulgaris (PV) is a life threatening autoimmune blistering disease characterized by loss of cell-cell adhesion of keratinocytes (acantholysis) and the formation of non-healing suprabasal intraepidermal blisters (1,2). Its annual incidence ranges from 0.098-5 patients per 100,000 individuals (3). Although the use of corticosteroids and immunosuppressive agents has markedly improved clinical outcomes in patients with PV, prolonged administration of these drugs increases the risk of serious adverse events, with infections being particularly notable (4). Growing evidence indicates that autoantibody-induced keratinocyte acantholysis involves multiple mechanisms. Autoantibodies binding to PV antigens not only directly disrupt desmosomal adhesive function but also activate intracellular kinase signaling pathways downstream of ligated antigens. These include epidermal growth factor receptor (EGFR), Src, mammalian target of rapamycin (mTOR), p38 mitogen-activated protein kinases (MAPK), as well as elevated intracellular calcium and activation of cell death cascades, leading to the dissociation of keratinocyte and formation of acantholysis (5). Therefore, uncovering the mechanisms by which autoantibodies trigger acantholysis and cell death is crucial for the development of targeted therapeutics.

Recently, increasing evidence has demonstrated that interleukins play significant roles and represent promising therapeutic targets in skin-related diseases (6,7). Our previous study found that interleukin-37 (IL-37) inhibits keratinocyte dissociation and desmoglein-3 (Dsg3) endocytosis through upregulating caveolin-1 and inhibiting signal transducer and activator of transcription 3 (STAT3) pathways (8). IL-37 is predominantly expressed in circulating monocytes, macrophages, dendritic cells,

tonsillar B cells, and plasma cells, as well as in epithelial cells of the skin and gut in response to inflammation (9). In psoriasis, IL-37 expression has been reported to be decreased (10); however, findings in atopic dermatitis remain inconsistent (9,11,12).

As a member of interleukin-1 superfamily, IL-37 functions as a natural suppressor of inflammatory and immune responses (13,14). It modulates both innate and acquired immunity by maintaining the cytokine balance away from excessive inflammation (15,16). Notably, IL-37 binds to the IL-18Rα and recruits the co-receptor IL-1R8 to form a tripartite complex, triggering a signaling cascade that involves mTOR, MAPK and NF-kB pathways (17). Johnston *et al* (18) identified synergistic interactions between IL-1 and EGFR, a pivotal regulator of epithelial homeostasis, in enhancing keratinocyte antimicrobial defense mechanisms. Furthermore, it has been demonstrated that PV-IgG induces EGFR activation, and clinical use of EGFR inhibitors such as lapatinib prevents keratinocyte blister formation (19). These findings led to the hypothesis that IL-37 may regulate EGFR-mediated keratinocyte acantholysis and cell death.

The present study stimulated HaCaT keratinocytes with anti-Dsg3 antibody to establish an *in vitro* PV model and co-cultured these cells with IL-37 to investigate its role and underlying mechanisms in PV pathogenesis. The results revealed that IL-37 treatment markedly reduced keratinocyte dissociation and apoptosis in anti-Dsg3 antibodies-treated-keratinocytes through the IL-1R8/TNF-alpha-converting enzyme (TACE/ADAM-17)/EGFR pathway. Collectively, these findings identified IL-37 as a pivotal regulator of EGFR activation and keratinocyte dissociation in PV, highlighting its potential as a therapeutic target.

Materials and methods

Collection of serum and skin tissues. Between June 2019 and June 2020, serum and skin tissues were collected from 15 patients with PV (8 males and 7 females; mean age 46.00±12.63 years, range 21-70) undergoing treatment in the Department of Dermatology in People's Hospital of Xinjiang Uygur Autonomous Region. Healthy control serum (15 samples, 7 males and 8 females; mean age 45.20±12.03 years, range 25-63) and skin tissues (5 samples) were collected from participants undergoing skin plastic surgery at the same hospital. The present study was approved by the Ethics Committee of the People's Hospital of Xinjiang Uygur Autonomous Region (approval no. 2019030616). The procedures followed were in accordance with the Helsinki Declaration of 1975, as revised in 1983.

Cell culture. HaCaT cells were obtained from Cell Bank of the Chinese Academy of Sciences (cat. no. SCSP-5091). The cell line has tested negative for mycoplasma, bacteria and fungi and has been verified by STR profiling. HaCaT cells were cultured in DMEM (Gibco; Thermo Fisher Scientific, Inc. Massachusetts, USA.) containing 10% fetal bovine serum (FBS; Gibco; Thermo Fisher Scientific, Inc.) at 37˚C and 5% CO_2 incubator.

CCK-8 assay. HaCaT cells ($2x10^3$ cell/well) were cultured in 96-well plate and treated with different concentration of IL-37 recombinant protein (0, 25, 50, 100, and 200 ng/ml). Then, 10 μl of CCK-8 (Beyotime Biotechnology) were added and cultured for 1 h, the absorbance were detected at 450 nm.

Construction of PV-cell model. To establish the *in vitro* model of antibody-induced acantholysis, HaCaT cells placed in 6-well plates were treated with mouse monoclonal anti-Dsg3 antibody AK23 (cat. no. MA5-51877; Thermo Fisher Scientific, Inc.) at a dilution of 1:2,000 or 1:1,000 for 24 h at 37˚C. Subsequently, the cells were treated with IL-37 recombinant protein (isoform b; 100 ng/ml; cat. no. 10155-HNAE; Sino Biological, Inc.) for 24 h at 37˚C.

Cell transfection and treatment. To knockdown the expression of IL-1R8, IL-18Rα and ADAM17, HaCaT cells were transfected with 50 nM of IL-1R8-, IL-18Rα- and ADAM17-specific small interference RNA (si-RNA; Shanghai GenePharma Co., Ltd.) using Lipofectamine® 3000 (Invitrogen; Thermo Fisher Scientific, Inc.) for 48 h at 37˚C according to the manufacturer's instructions. The knockdown efficiency was detected by western blot assay. Subsequently, HaCaT cells were treated with AK23 for 24 h and 100 ng/ml of IL-37 recombinant protein for another 24 h. The sequences of siRNAs were as follows: si-IL-1R8 #1: 5'-GCAAGUUCGUGAACUUCAUCC -3', and 5'-AUGAAGUUCACGAACUUGCGG-3'; si-IL-1R8 #2: 5'-GCGUCGCUCCUCUGCUCAACA -3', and 5'-UUG AGCAGAGGAGCGACGCCG'; si-IL-1R8 #3: 5'-GGGAGA GUUUGCUCCCAAAGG-3', and 5'-UUUGGGAGCAAA CUCUCCCCU-3'; si-IL-18R #1: 5'-GAGUGAGAUUGUCAG UGUAAG -3' and 5'-UACACUGACAAUCUCACUCUU -3'; si-IL-18R #2: 5'-GAGUCUUAAUCUUCAGAAACA -3' and 5'-UUUCUGAAGAUUAAGACUCGG -3'; si-IL-18R #3: 5'-GAGAAGAGAUGAAACAUUAAC-3' and 5'-UAAUGU UUCAUCUCUUCUCGU -3'; si-ADAM17 #1: 5'-GAUUUG ACCUACAAAUCAAUC-3' and 5'-UUGAUUUGUAGGUCA AAUCUA -3'; si-ADAM17 #2: 5'-AGAGAUCUACAGACU UCAACA -3' and 5'-UUGAAGUCUGUAGAUCUCUUU -3'; si-ADAM17 #3: 5'-GAAUCGUGUUGACAGCAAAGA -3' and 5'-UUUGCUGUCAACACGAUUCUG -3'; si-NC: 5'-UUC UCCGAACGUGUCACGUTT -3' and 5'-ACGUGACACGUU CGGAGAATT-3'.

For EGFR inhibition assay, HaCaT cells were pre-treated with 1 μM of EGFR inhibitor AG1478 (MedChemExpress) at 37˚C for 30 min followed by treatment with AK23 for 24 h at 37˚C.

Enzyme-linked immunosorbent assay (ELISA). The levels of IL-37 (cat. no. PI652), IL-6 (cat. no. PI325), IL-10 (cat. no. PI536), and IL-17 (cat. no. PI550) in the serum or cellular supernatant were measured using ELISA kits (Beyotime Biotechnology) according to the manufacturer's instructions. Briefly, the serum (50 μl sample analysis buffer and 50 μl serum/well) or cellular supernatant (100 μl/well) was added and cultured for 120 min at room temperature. Then, biotinylated antibody (100 μl/well) was added and cultured for 60 min at room temperature. Following this, streptavidin (100 μl/well) labeled with horseradish peroxidase was added and incubated at room temperature for 20 min away from light. Then, a color-developing agent (TMB solution; 100 μl/well) was added, and the reaction wells were sealed using a sealing plate

film (white), and incubated at room temperature for 15 min away from light. Finally, a termination solution (50 μl/well) was added and the absorbance was measure at 450 nm immediately after mixing.

Immunohistochemical staining. Skin tissues were fixed with 4% paraformaldehyde for 15 min at room temperature, and then permeabilized with 0.5% Triton X-100 for 20 min at room temperature. After blocking with normal goat serum in PBS containing 0.1% Tween for 30 min at room temperature, the tissue sections were incubated with IL-37 antibody (cat. no. ab278499; Abcam) overnight at 4˚C. The next day, the skin tissues were incubated with biotin-labeled goat anti-rabbit IgG (H+L) antibody (Thermo Fisher Scientific, Inc.; 1:200) for 15 min at room temperature. They were then counterstained with hematoxylin for 5 min at room temperature. Finally, images of the skin tissue sections were captured using a light microscope (Leica DM4000 B LED; Leica Microsystems GmbH).

Dsg3 immunocytofluorescence. HaCaT keratinocytes cultured with or without mouse anti-Dsg3 antibody (1:1,000 dilution) were fixed with 4% paraformaldehyde, incubated with 0.1% Triton X-100 for 10 min at room temperature and then blocked with 5% goat serum for 1 h at room temperature. Subsequently, mouse anti-Dsg3 antibodies (1:100 dilution; cat. no. NBP1-78984; Novus Biologicals; Bio-Techne) were added and incubated at 4˚C. The next day, Alexa Fluor 594-labelled goat anti-rabbit IgG (cat. no. 33112ES60; Shanghai Yeasen Biotechnology Co., Ltd.) was added and incubated for another 2 h at 37˚C in the dark. The nuclei were stained with DAPI at room temperature for 5 min (1:5,000 dilution; Beyotime Biotechnology). Images of fluorescence staining were captured using a fluorescence microscope.

Reverse transcription-quantitative (RT-q) PCR. Cells ($1x10^6$ cell) were collected and lysed with TRIzol® reagent (Invitrogen; Thermo Fisher Scientific, Inc.), after which their RNA was extracted. RNA (1 μg) was reverse transcribed into the cDNA using the PrimeScript RT Master Mix kit (Takara Biotechnology Co., Ltd.) following the manufacturer's instructions. The mRNA levels of these samples were then detected using SYBR® Premix Ex Taq II (Qiagen China Co., Ltd.) according to the manufacturer's instructions. The reactions program was as follows: 95˚C for 5 min, followed by 40 cycles at 95˚C for 5 sec and 60˚C for 34 sec and finally extended at 72˚C for 10 min. Gene expression levels were quantified using the $2^{-\Delta\Delta Cq}$ method (20), with β-actin serving as the endogenous reference gene. The primers used were: IL-37: Forward: 5'-GACCAGGATCACAAAGTACTGG -3', Reverse: 5'-GAGCTCAAGGATGAGGCTAATG -3'; IL-10: Forward: 5'-GCTGGAGGACTTTAAGGGTTAC -3', Reverse: 5'-GATGTCTGGGTCTTGGTTCTC -3'; IL-6: Forward: 5'-CACTCACCTCTTCAGAACGAAT -3', Reverse: 5'-GCTGCTTTCACACATGTTACTC -3'; IL-17: Forward: 5'-GAAATCCAGGATGCCCAAATTC -3', Reverse: 5'-GAGGTGGATCGGTTGTAGTAATC -3'; β-actin: Forward: 5'-AGCCTTCCTTCCTGGGCAT -3', Reverse: 5'-TGATCTTCATTGTGCTGGGTG -3'. All experiments were performed in three independent biological replicates.

Western blotting. All the cell samples from all the groups and the skin tissue samples from patients with PV were lysed with RIPA buffer (cat. no. P0013C; Beyotime Biotechnology,) for 10 min at 4˚C. Protein concentration was determined using the Bradford Protein Concentration Assay Kit (Beyotime Biotechnology). Total protein (20 μg) were electrophoresed on 6, 8, 10 or 12% SDS-PAGE gel and subsequently transferred to a PVDF membrane. The membranes were then blocked using a blocking buffer (Beyotime Biotechnology) for 1 h at room temperature. Following this, the membranes were incubated with the following specific primary antibodies overnight at 4˚C: Rabbit anti-IL-37 monoclonal antibody (cat. no. ab278499; Abcam), rabbit anti-Bax monoclonal antibody (cat. no. ab32503; Abcam), rabbit anti-Bcl-2 polyclonal antibody (cat. no. ab59348; Abcam), rabbit anti-caspase 3 antibody (cat. no. 9662; Cell Signaling Technology, Inc.), rabbit anti-cleaved caspase3 antibody (cat. no. 9661; Cell Signaling Technology, Inc.), mouse anti-IL-1R8 antibody (cat. no. sc-271864; Santa Cruz Biotechnology, Inc.), mouse anti-IL-18Rα antibody (cat. no. PA5-115404; Thermo Fisher Scientific, Inc.), rabbit anti-EGFR phospho Y1173 antibody (cat. no. ab5652; Abcam), rabbit anti-EGFR antibody (cat. no. ab52894; Abcam), rabbit anti-ADAM17 polyclonal antibody (cat. no. ab39162; Abcam), anti-phosphorylated (p-) ERK1/2 antibody (cat. no. ab201015; Abcam), anti-ERK1/2 antibody (cat. no. ab184699; Abcam), anti-p-AKT (Ser473) antibody (cat. no. 9271; Cell Signaling Technology, Inc.), anti-AKT antibody (cat. no. 4691; Cell Signaling Technology, Inc.), anti-p-STAT3 antibody (cat. no. ab76315; Abcam), and anti-STAT3 antibody (cat. no. ab68153; Abcam). Then, the appropriate HRP-conjugated goat anti-rabbit IgG or goat anti-mouse antibodies were added and incubated for 1 h at room temperature. Finally, positive bands were visualized using an imaging system (Bio-Rad Laboratories, Inc.). Densitometric analysis was performed using ImageJ software (version 1.53; National Institutes of Health).

Dispase-based dissociation assay. HaCaT keratinocytes were cultivated on 24-well plates at a density of $1x10^6$ per well. The cells were then stimulated with or without anti-Dsg3 antibody in the presence or absence of IL-37 and/or EGFR activator NSC228155 for 15 min at 37˚C. After two washes using phosphate-buffered saline (PBS), each well was treated with 2 U/ml of Dispase II (MilliporeSigma) and incubated at 37˚C for 30 min. Dispase II was then gently removed, and 1 ml of PBS was added. The cells were then pipetted up and down 10 times using a 1 ml electric pipette at a constant speed to disrupt the integrity of the monolayer cells and dissociate the cells. Finally, cell debris was stained with 0.01% crystal violet (MilliporeSigma) at room temperature for 1 min and the number of fragments was measured using an inverted microscope. The experiment was performed three times.

Mitochondrial membrane potential. The PV-cell model was treated with IL-37 recombinant protein for 24 h, after which it was washed twice with PBS. The cells were then stained with 1.0 mM of JC-1 (cat. no. C2005; Beyotime Biotechnology) at 37˚C for 10 min. The fluorescence intensity of the cells was detected using a fluorescence microscope.

Flow cytometry. All the groups of cells were washed with PBS for three times and then double-stained with annexin V-FITC and propidium iodide at 37˚C for 20 min. The apoptosis of each sample group was analyzed using a fluorescence-activated cell sorter (FACS; CytoFLEX; Beckman Coulter, Inc.). Data analysis was conducted using FlowJo software (version 10.8.1; Becton, Dickinson & Company, Oregon, USA). Apoptotic rates were calculated as the sum of the percentage of early and late apoptotic cells.

Co-immunoprecipitation assays. Co-immunoprecipitation assays were conducted according to the manufacturer's instructions (cat. no. 88804, Thermo Fisher Scientific, Inc.) The HaCaT cells were washed with PBS and lysed with lysis buffer (0.025M pH=7.4 Tris, 0.15M NaCl, 0.001M EDTA, 1% NP40 and 5% glycerol) supplemented with a protease inhibitor cocktail (100: 1 (v/v)). After being centrifuged at 13,680 x g for 15 min at 4˚C, the supernatant was collected, and 20 μl of the collected supernatant was used as input. The remaining cell lysate supernatant (0.5 mg per reaction) was incubated with 2 μg of IL-37 antibody (cat. no. ab278499; Abcam, IgG antibody was used as control) at 4˚C overnight. The immunocomplex was captured using 10 μl of protein A+G beads at 37˚C for 1 h. After incubation, the complex was separated on a magnetic rack for 10 sec, and then washed thrice using wash buffer (0.025 M pH=7.4 Tris, 0.15 M NaCl, 0.001 M EDTA, 1% NP40 and 5% glycerol) supplemented with a protease inhibitor cocktail. Western blotting was used for further analysis.

Statistical analysis. The data were analyzed using SPSS 18.0 (SPSS, Inc.) and GraphPad Prism 6 (Dotmatics) and expressed as mean ± SD. Differences between two groups were estimated by independent sample t test. Differences among multiple groups were estimated using one-way ANOVA with Bonferroni's post-hoc test. The correlations between serum IL-37 and IL-10, IL-6, and IL-17, respectively, were assessed using Pearson's correlation analysis. All experiments were conducted with three independent biological replicates. A post hoc power analysis was conducted using G*Power 3.1.9.2 (Heinrich Heine University Düsseldorf, Düsseldorf, Germany) to evaluate the sufficiency of the clinical sample size. Given α=0.05, n=15 per group, and IL-37 concentrations of 4.20± 0.98 pg/ml (healthy control) vs. 10.52±2.87 pg/ml (PV), the achieved power was 1.00, which exceeds the conventional threshold of 0.9. $P<0.05$ was considered to indicate a statistically significant difference.

Results

IL-37 is augmented in PV and associated with inflammatory factors. To elucidate the pathophysiological role of IL-37 in PV, the present study analyzed the concentration of IL-37 in the serum and skin tissues from healthy controls and. Serum IL-37 levels were markedly higher in patients with PV compared with healthy controls (Fig. 1A). Similarly, IL-37 expression was markedly elevated in the skin tissues of patients with PV than in healthy controls, as indicated by immunohistochemistry assays (Fig. 1B and C). Furthermore, serum IL-37 levels showed a positive correlation with the anti-inflammatory factor IL-10 (Fig. 1D), and a negative correlation with the pro-inflammatory cytokines IL-6 and IL-17 (Fig. 1E and F).

IL-37 protects HaCaT cells from Dsg3-induced keratinocyte dissociation and apoptosis. To investigate the functional role of IL-37 in PV, an *in vitro* PV model was established by treating HaCaT keratinocytes with the anti-Dsg3 antibody AK23. Immunofluorescence staining revealed that under control or with a low anti-Dsg3 antibody (1:2,000 dilution) treated conditions, Dsg3 exhibited a linear, continuous staining along the cell borders. By contrast, a higher anti-Dsg3 antibody concentration (1:1,000 dilution) resulted in markedly reduced Dsg3 staining, indicating impaired cell adhesion and successful modeling of PV-like acantholysis (Fig. 2A). HaCaT cells were treated with different concentration of IL-37 recombinant protein (0, 25, 50, 100 and 200 ng/ml). As shown in Fig. 2B, IL-37 at concentrations of 100 ng/ml and below had no effect on cell viability, whereas 200 ng/ml IL-37 markedly reduced cell viability. Therefore, 100 ng/ml IL-37 was selected for subsequent experiments. The anti-Dsg3 antibody treatment markedly increased the IL-37 levels (Fig. 2B and C). Co-treatment with 100 ng/ml of IL-37 and anti-Dsg3 antibody further enhanced IL-37 expression compared with anti-Dsg3 antibody alone (Fig. 2C and D). Additionally, the concentration and mRNA expression of IL-10 were markedly increased (Fig. 2E and F), while the concentration and mRNA expression of IL-6 (Fig. 2G and H) and IL-17 (Fig. 2I and J) were markedly decreased in IL-37 in combination with the anti-Dsg3 treated HaCaT group.

The dispase-based dissociation assays demonstrated a significant increase in the number of fragments in the anti-Dsg3 group compared with the control group (Fig. 3A). By contrast, IL-37 treatment reduced the number of fragments compared with the anti-Dsg3 group (Fig. 3A). Given that PV pathogenesis may be initiated by pro-apoptotic proteins and that the apoptotic pathway are activated prior to morphological signs of acantholysis (21,22), the present study further analyzed the apoptosis of the HaCaT cells. JC-1 assay revealed enhanced green fluorescence and reduced red fluorescence in the anti-Dsg3 group compared with the control group, indicating a transition from red to green fluorescence, characteristic of early apoptosis in the anti-Dsg3 group (Fig. 3B). However, IL-37 decreased the intensity of green fluorescence and increased the red fluorescence intensity, suggesting that IL-37 treatment increased mitochondrial membrane potential and inhibited cell apoptosis (Fig. 3B). Consistent with these findings, the flow cytometry analysis demonstrated that the apoptosis of HaCaT cells was increased in the anti-Dsg3 group compared with the control group, whereas the apoptosis of HaCaT cells in the anti-Dsg3+IL-37 group was decreased compared with that in the anti-Dsg3 group (Fig. 3C). Further analysis of apoptosis-related markers showed that anti-Dsg3 antibody exposure markedly decreased Bcl-2 expression and increased expression of Bax and cleaved-caspase 3 compared with the control group (Fig. 3D-G). IL-37 treatment reversed these changes, upregulating Bcl-2 and downregulating Bax and cleaved-caspase 3 expression (Fig. 3D-G).

IL-37 protects HaCaT cells from keratinocyte dissociation and apoptosis through IL-1R8. As a ligand protein, IL-37

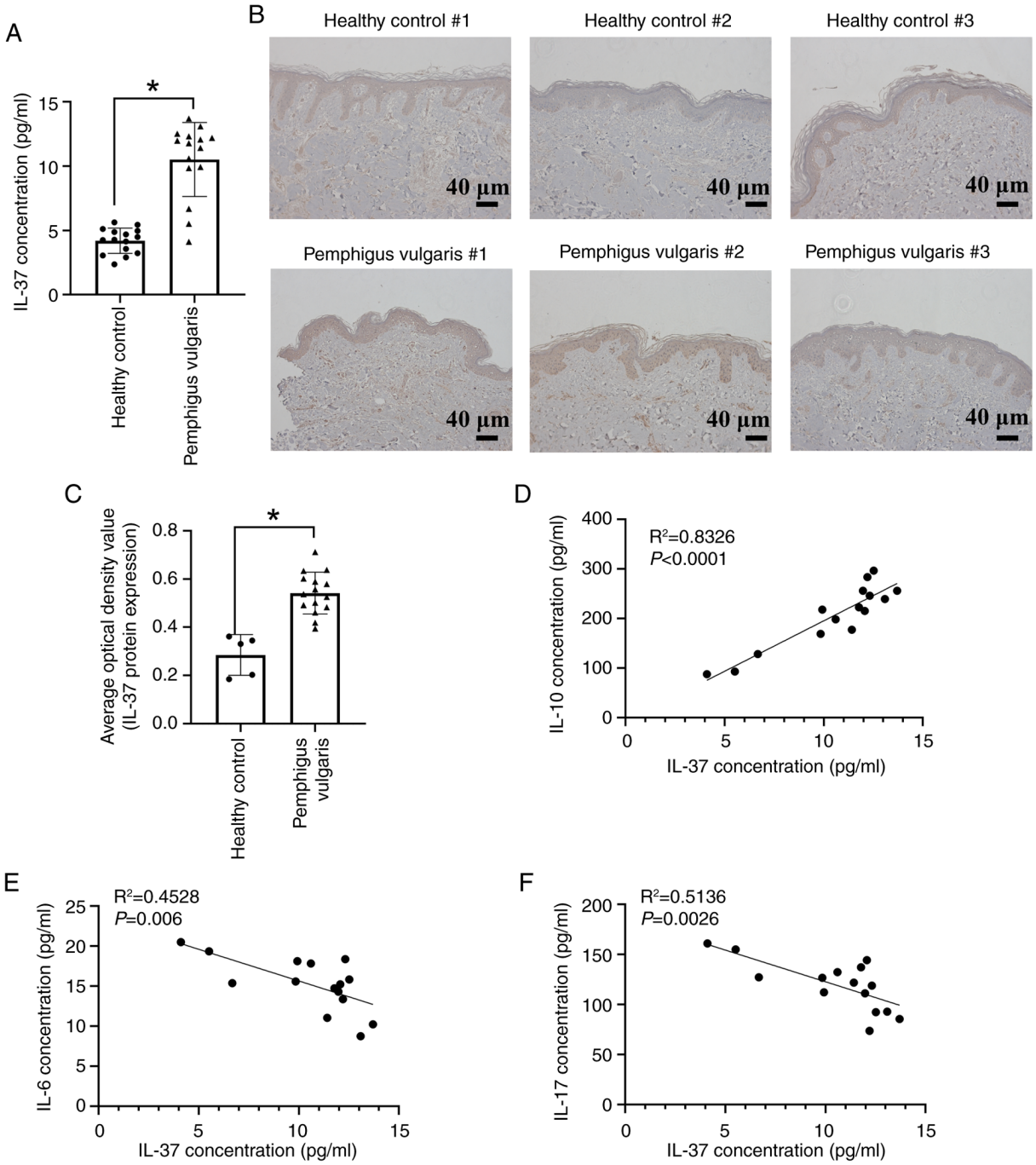

Figure 1. IL-37 was augmented in pemphigus vulgaris and associated with inflammatory factor. (A) IL-37 concentration in the serum of healthy controls (n=15) and patients with pemphigus vulgaris (n=15) was detected by ELISA assay. Data are presented as mean ± SD. (B and C) IL-37 expression in skin tissue of healthy control and pemphigus vulgaris was analyzed by immunohistochemistry. (D) The correlation between serum IL-37 and IL-10 levels was assessed using Pearson's correlation analysis. (E) The correlation between IL-37 and IL-6 levels was assessed using Pearson's correlation analysis. (F) The correlation between IL-37 and IL-17 levels was assessed using Pearson's correlation analysis. *P<0.05. IL, interleukin; ELISA, enzyme-linked immunosorbent assay.

functions by binding to its receptor IL-1R8 (23). The co-immunoprecipitation assay confirmed the interaction of IL-37 and IL-1R8 in the HaCaT cells (Fig. 4A). To further investigate the functional role of this interaction, IL-1R8 and IL-18Rα were knocked down in the HaCaT cells through transfection with IL-1R8-specific siRNA and IL-18Rα-specific siRNA, respectively. IL-1R8 and IL-18Rα expression were markedly decreased in IL-1R8 siRNA (Fig. 4B) or IL-18Rα siRNA (Fig. 4C) transfected HaCaT cells. Knockdown of either IL-1R8 or IL-18Rα resulted in an increased number of cellular fragments compared with the negative control siRNA transfected HaCaT cells (Fig. 4D). Additionally, the apoptosis rate was markedly higher in the anti-Dsg3 + IL-37 + si-IL-1R8 group and anti-Dsg3 + IL-37 + si-IL-18Rα group than in the anti-Dsg3 + IL-37 + si-NC group (Fig. 4E and F). Consistent with these findings, the Bax expression was upregulated, while the Bcl-2 expression was downregulated in the anti-Dsg3 + IL-37 + si-IL-1R8 group and anti-Dsg3 + IL-37 + si-IL-18Rα group relative to the anti-Dsg3 + IL-37 + si-NC group (Fig. 4G).

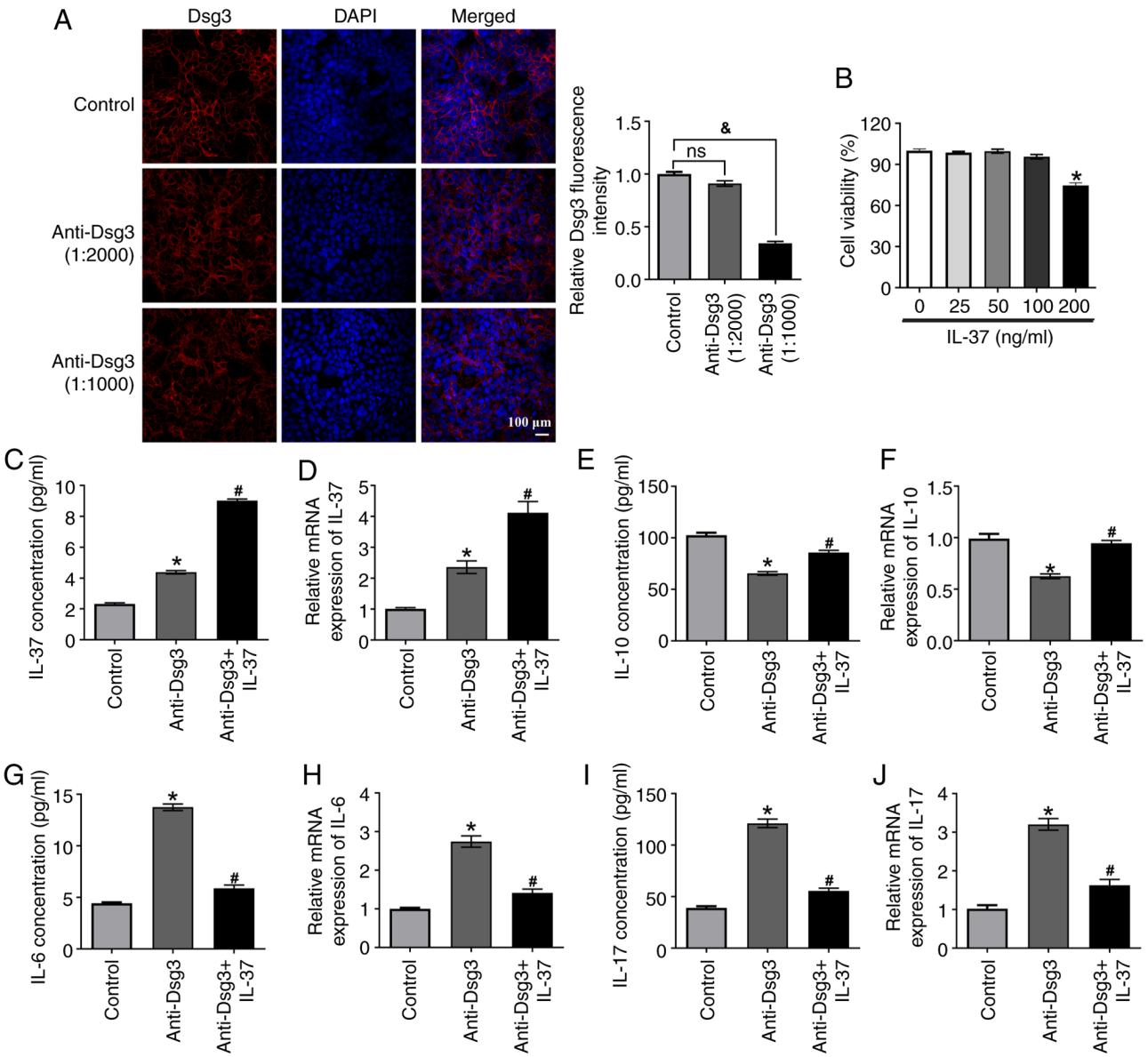

Figure 2. IL-37 protects HaCaT cells from Dsg3-induced keratinocyte dissociation and apoptosis. (A) The effect of different dilutions of Dsg-3 antibodies on cell dissociation was analyzed by immunofluorescence. (B) HaCaT cells were treated with different concentration of IL-37 recombinant protein (0, 25, 50, 100, and 200 ng/ml). Cell viability was detected by CCK-8 assay. (C) HaCaT cells were treated with the Dsg-3 antibodies, followed by administration of the IL-37 recombinant protein. The concentration of IL-37 was analyzed using an ELISA assay. (D) The relative mRNA expression of IL-37 was detected using RT-qPCR. The (E) concentration and (F) relative mRNA expression of IL-10 were measured using an IL-10 ELISA kit and RT-qPCR, respectively. The (G) oncentration and (H) relative mRNA expression of IL-6 were measured by the IL-6 ELISA kit and RT-qPCR, respectively. The (I) concentration and (J) relative mRNA expression of IL-17 were measured by the IL-17 ELISA kit and RT-qPCR, respectively. $^{\&}$P<0.05; *P<0.05 vs. Control group; $^{\#}$P<0.05 vs. anti-Dsg3 group. Data are presented as mean ± SD, n=3 biological independent replicates. One-way ANOVA with Bonferroni's post-hoc test was used for multiple group comparisons. IL, interleukin; Dsg3, desmoglein-3; ELISA, enzyme-linked immunosorbent assay; RT-qPCR, reverse transcription-quantitative PCR.

IL-37/IL-1R8 protects HaCaT cells from keratinocyte dissociation and apoptosis through the ADAM17/EGFR pathway. Following PV-IgG treatment, EGFR auto-phosphorylation, internalization and acantholysis were induced (24). It has been reported that IL-1R deficiency upregulates the expression of ADAM-17, a metalloproteinase responsible for the shedding and release of EGFR ligands (25). To further explore the potential mechanisms by which IL-37 administration induces keratinocyte dissociation and apoptosis, the present study examined the expression of ADAM17 and EGFR phosphorylation. Compared with the anti-Dsg3 group, ADAM17 expression, p-EGFR as well as EGFR downstream protein p-AKT, p-ERK1/2, and p-STAT3 levels were markedly decreased in the anti-Dsg-3 + IL-37 group, indicating a suppression of canonical EGFR signaling cascades (Fig. 5A). Furthermore, knockdown of IL-1R8 markedly increased the expression of ADAM17, p-EGFR, p-ERK1/2, p-AKT, and p-STAT3 levels in the anti-Dsg3 + IL-37 + si-IL-1R8 group when compared with that in the anti-Dsg3 + IL-37 + si-NC group (Fig. 5A).

Pharmacologically activation of EGFR using the EGFR activator NSC228155 enhanced epidermal fragment formation and apoptosis rates (Fig. 5B and C). Additionally, Bcl-2 expression was markedly decreased, whereas Bax protein expression was markedly increased in the anti-Dsg3 + IL-37 + NSC228155 group compared with the anti-Dsg3 + IL-37 group (Fig. 5D).

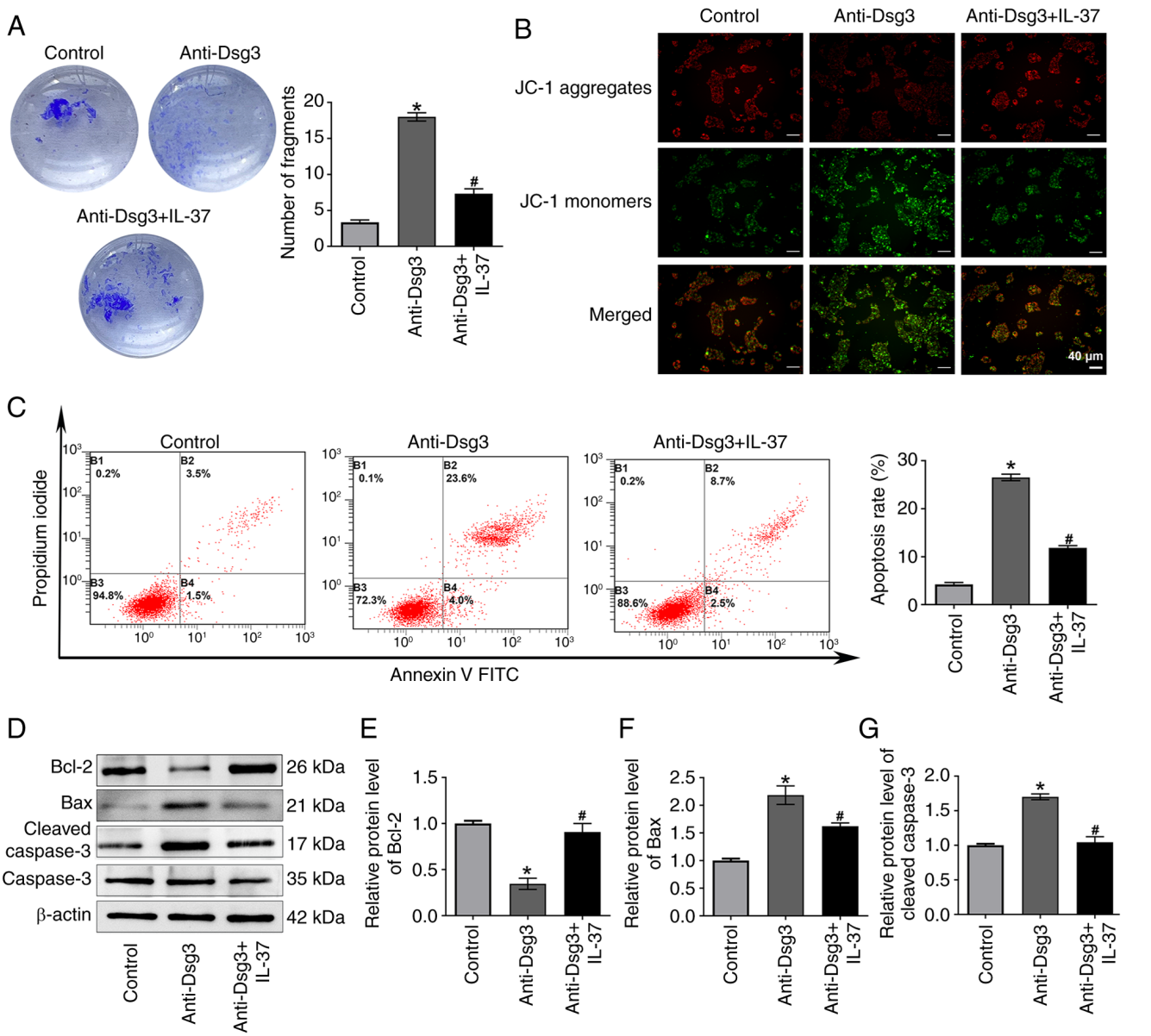

Figure 3. IL-37 protects HaCaT cells from keratinocyte dissociation and apoptosis. (A) The effect of IL-37 on cell dissociation was evaluated using a cell dissociation assay. (B) Mitochondrial membrane potential was assessed by JC-1 staining. (C) Cell apoptosis was analyzed by flow cytometry. (D) Protein expression levels of Bcl-2, Bax, Cleaved-caspase 3 and Caspase 3 were determined by western blotting. Quantitative analysis of (E) Bcl-2, (F) Bax and (G) Cleaved-caspase 3 protein levels. *P<0.05 vs. Control group; #P<0.05 vs. anti-Dsg3 group. Data are presented as mean ± SD, n=3 biological independent replicates. One-way ANOVA with Bonferroni's post-hoc test was used for multiple group comparisons. IL, interleukin.

Subsequently, HaCaT was transfected with ADAM17 siRNA and western blotting showed a downregulation of ADAM17 after ADAM17 siRNA transfection, with ADAM17 siRNA #1 demonstrating the most pronounced reduction in protein level (Fig. 5E). This ADAM17 knockdown markedly decreased both epidermal fragment formation (Fig. 5F) and apoptosis rates (Fig. 5G) compared with anti-Dsg3+si-NC group. Notably, compared with the anti-Dsg3 group, EGFR inhibitor AG1478 also decreased epidermal fragment formation and apoptosis rates (Fig. 5F and G).

Discussion

The present study demonstrated that IL-37 is highly expressed in the serum and skin tissue of patients with PV. IL-37 regulates HaCaT cell dissociation and apoptosis in an IL-1R8-dependent manner. Furthermore, the IL-37/IL-1R8 axis inhibits HaCaT cell dissociation and apoptosis by negatively regulating the ADAM17/EGFR pathway.

It is well established that desmoglein-1 (Dsg1) and Dsg3, calcium-dependent cell adhesion molecules, serve as the primary autoantibodies targets in the pathogenesis of PV (26). Several non-Dsg antigens, including desmocollin 1 and 3, mitochondrial proteins, human leukocyte antigen molecules and various subtypes of nicotinic and muscarinic acetylcholine receptor, have also been implicated in PV (27), indicating a multifactorial etiology. In a previous study, we found that IL-37 inhibited keratinocyte dissociation and Dsg3 endocytosis by upregulating caveolin-1 and inhibiting the STAT3 pathway (8). The present study discovered that IL-37 recombination protein

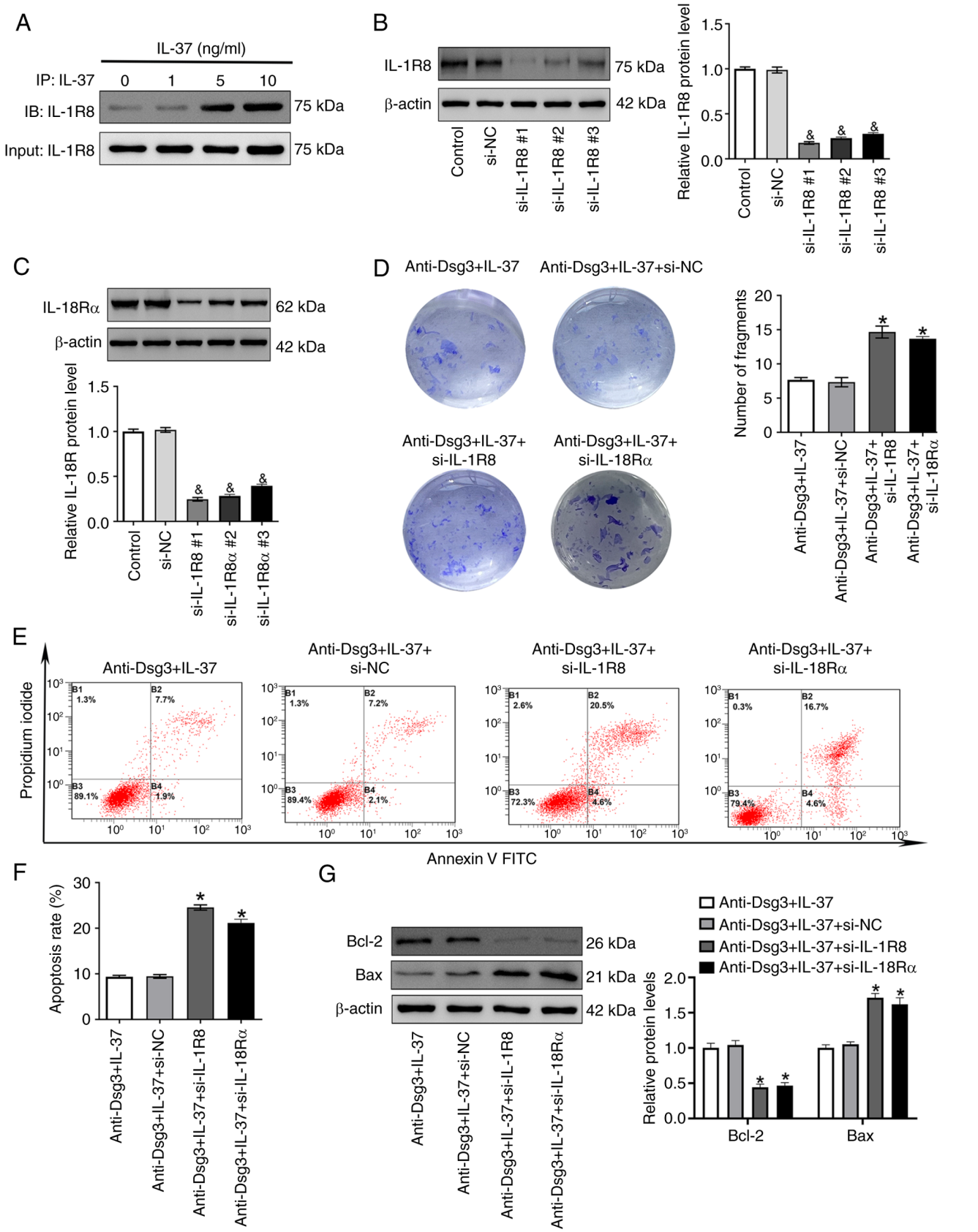

Figure 4. IL-37/IL-1R8 protects HaCaT cells from keratinocyte dissociation and apoptosis through the ADAM17/EGFR pathway. (A) The interaction between IL-37 and IL-1R8 was analyzed using co-immunoprecipitation. (B) HaCaT cells were transfected with IL-1R8 siRNA and the transfection efficiency were detected by western blotting. (C) HaCaT cells were transfected with IL-18Rα siRNA and the transfection efficiency were detected by western blotting. (D) IL-1R8 siRNA or IL-18Rα transfected HaCaT were treated with anti-Dsg-3 and IL-37 recombinant protein. The number of fragments was analyzed by cell dissociation assay. (E and F) Cell apoptosis was analyzed by flow cytometry. (G) Protein expression levels of Bcl-2 and Bax were determined by western blotting. $^{\&}$P<0.05 vs. si-NC; *P<0.05 vs. anti-Dsg3 + IL-37 + si-NC group. Data are presented as mean ± SD, n=3 biological independent replicates. One-way ANOVA with Bonferroni's post-hoc test was used for multiple group comparisons. IL, interleukin; ADAM17, TNF-alpha-converting enzyme; EGFR, epidermal growth factor receptor; si, short interfering.

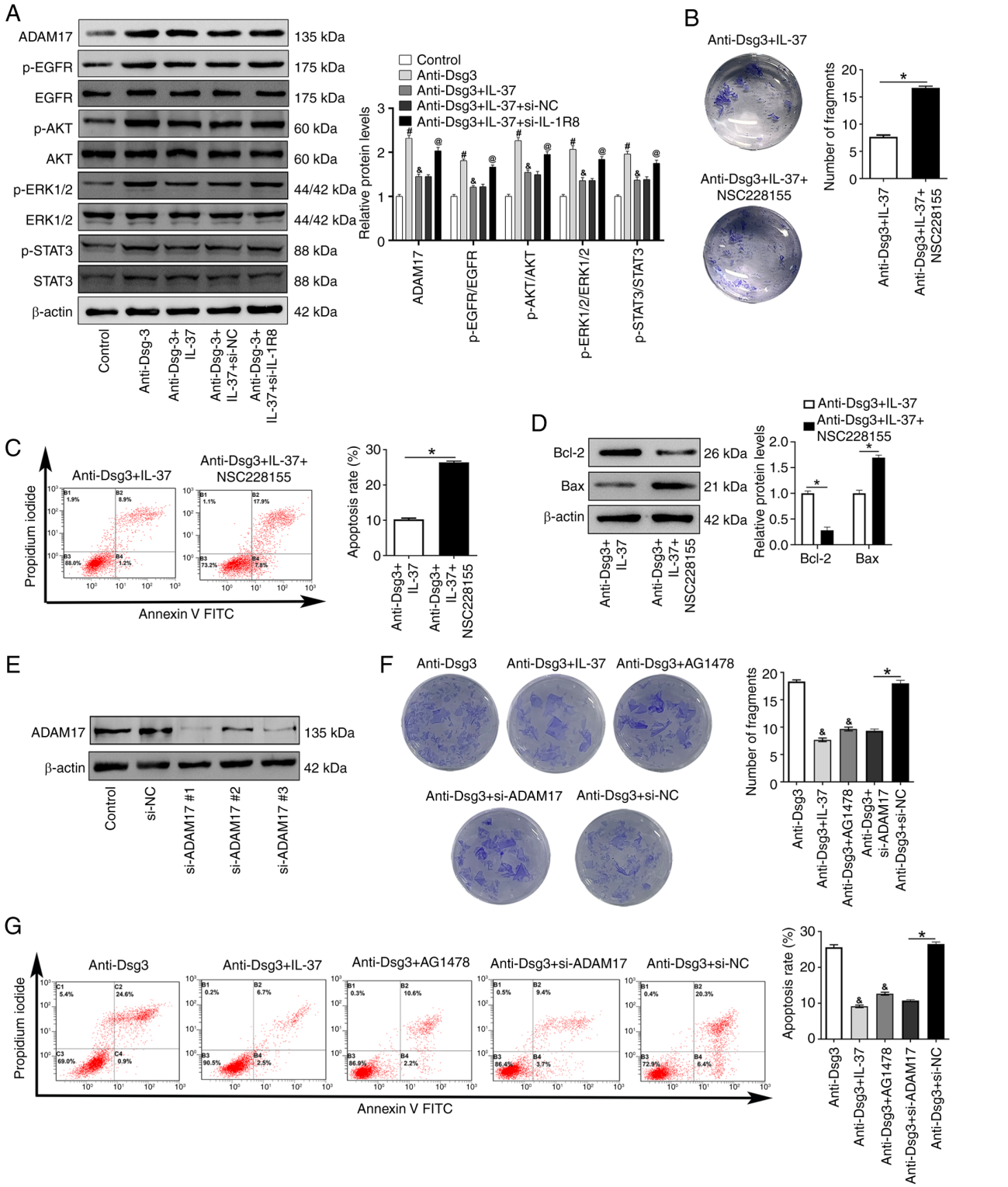

Figure 5. IL-37/IL-1R8 protects HaCaT cells from keratinocyte dissociation and apoptosis through the ADAM17/EGFR pathway. (A) Protein expression levels of ADAM17, p-EGFR, total EGFR as well as EGFR downstream protein p-AKT, p-ERK1/2 and p-STAT3 levels were determined by western blotting. HaCaT cells were treated with EGFR activator NSC228155. (B) Cell dissociation was analyzed by cell dissociation assay. (C) Cell apoptosis was analyzed by flow cytometry. (D) Protein expression levels of Bcl-2 and Bax were analyzed by western blotting. (E) HaCaT was transfected with ADAM17 siRNA and the transfection efficiency was detected by western blotting. HaCaT cells were transfected with ADAM17 siRNA or treated with 1 μM of EGFR inhibitor AG1478 for 30 min followed by treated with AK23. (F) Cell dissociation was analyzed by cell dissociation assay. (G) Cell apoptosis was analyzed by flow cytometry. $^{\#}$P<0.05 vs. Control group; $^{\&}$P<0.05 vs. anti-Dsg3 group; $^{@}$P<0.05 vs. anti- Dsg3 + IL-37 + si-NC group; *P<0.05; Data are presented as mean ± SD, n=3 biological independent replicates. One-way ANOVA with Bonferroni's post-hoc test was used for multiple group comparisons. IL, interleukin; ADAM17, TNF-alpha-converting enzyme; EGFR, epidermal growth factor receptor; p- phosphorylated; STAT, signal transducer and activator of transcription; si, short interfering.

led to a loss of cell dissociation and a decrease in cell apoptosis. As a ligand protein, IL-37 functions by binding to its receptors, IL-1R8 and IL-18R. Previous reports indicate that IL-37b exerts anti-inflammatory effects through IL-1R8 by

inhibiting the p38, ERK, JNK, and NF-κB pathways, and that IL-1R8 knockdown impairs the anti-inflammatory activity of IL-37 (28,29). Using a co-immunoprecipitation assay, the present study confirmed the interaction between IL-37 and IL-1R8. Knockdown of IL-1R8 reversed the protective effect of IL-37 on cell dissociation and apoptosis, suggesting that IL-37 acts through an IL-1R8-dependent mechanism.

Following PV IgG treatment, EGFR autophosphorylation, internalization and acantholysis are induced (24). In keratinocytes, inhibition of EGFR blocked PV IgG-triggered Dsg3 endocytosis, keratinocyte dissociation and blister formation, indicating cross-talk between EGFR and Dsg3 (24). Various factors, including G-protein-coupled receptor agonists and cytokines (such as IL-1β), can transactivate EGFR. This transactivation requires ADAM-17, a metalloproteinase that mediates the shedding and release of EGFR ligands (30). Previous studies have demonstrated that ADAM family members are associated with cell adhesion (31) and, specifically, ADAM10 and ADAM17 contribute to Dsg2 turnover (32). Additionally, ADAM17 can be activated by interleukin-15 (33). Notably, Wang *et al* (25) reported that IL-1R deficiency increased ADAM17 expression levels in a rat model of Alzheimer's disease. The present study found that IL-37 markedly decreased both ADAM17 expression and EGFR phosphorylation. Furthermore, activation of EGFR reversed the effects of IL-37 on HaCaT cell dissociation and apoptosis. It is well established that patients with PV exhibit a distinct autoantibody profile, leading to variations in intracellular signaling patterns (27,34). For instance, patients with PV and with anti-Dsg3 and anti-Dsg1 antibodies, but not anti-desmocollin3 antibodies, show increased levels of EGFR ligands such as EGF. These patients can benefit from treatment with EGF or EGFR inhibitors (34). Thus, patients with PV and with DSG1/3 antibodies might respond favorably to IL-37 therapy. Importantly, the function of IL-37 is concentration-dependent; at high concentrations, it forms dimers that inactivate it, thus inhibiting its anti-inflammatory function (35). This crucial mechanism underscores that its function is not linear. In the present study, the observed IL-37 levels appeared to fall within a therapeutic window where its net effect remained protective. Future studies are warranted to delineate the exact concentration threshold for dimerization in PV and to explore IL-37 as a potential therapeutic agent, where strategies to stabilize its active, monomeric form could be highly beneficial. Therefore, the concentration of IL-37 must be carefully considered in clinical applications aiming to inhibit EGFR in PV.

The present study used an anti-Dsg3 antibody (AK23) induced HaCaT cell model. However, this model does not fully recapitulate the complexity of PV, which involves multiple autoantibodies and patient heterogeneity. Validating key findings in a murine model of PV or patient-derived samples is needed in further studies.

In conclusion, the present study demonstrated that IL-37 inhibited ADAM17-mediated EGFR activation via its receptor IL-1R8, thereby inhibiting keratinocyte acantholysis and apoptosis. These findings provide new perspective on the treatment of pemphigus, suggesting that therapeutic strategies may extend beyond small-molecule EGFR inhibitors to include targeting the IL-37/IL-1R8 pathway.

Acknowledgements

Not applicable.

Funding

The present study was supported by National Natural Science Foundation of China (grant no. 82260621), Natural Sciences of Xinjiang Uygur Autonomous Region (grant no. 2022D01C623) and Basic and Clinical Research Project of Stem Cell Biotherapy-People's Hospital of Xinjiang Uygur Autonomous Region (grant no. GXBZX-2023004).

Availability of data and materials

The data generated in the present study may be requested from the corresponding author.

Author' contributions

FH was responsible for formal analysis, methodology, supervision, original draft preparation, writing, reviewing and editing. WC was responsible for formal analysis, supervision, original draft preparation, writing, reviewing and editing. QW was responsible for formal analysis and methodology. XZ was responsible for formal analysis and methodology. FX was responsible for formal analysis and methodology. JZ was responsible for conceptualization, supervision, writing, reviewing and editing. JL was responsible for conceptualization, supervision, writing, reviewing and editing.

Ethics approval and consent to participate

The present study was approved by the Ethics Committee of the People's Hospital of Xinjiang Uygur Autonomous Region (approval no. 2019030616). The procedures followed were in accordance with the Helsinki Declaration of 1975, as revised in 1983. Serum and skin tissues were collected from 15 patients with PV who were undergoing treatment in the Department of Dermatology in People's Hospital of Xinjiang Uygur Autonomous Region. Serum (15 samples) and skin tissue (5 samples) from healthy control were collected from participants who were undergoing skin plastic surgery in plastic surgery in the same hospital.

Patient consent for publication

Not applicable.

Competing interests

The authors declare that they have no competing interests.

References

1. Vafaeian A, Mahmoudi H and Daneshpazhooh M: What is novel in the clinical management of pemphigus vulgaris? Expert Rev Clin Pharmacol 17: 489-503, 2024.
2. Schmidt E, Kasperkiewicz M and Joly P: Pemphigus. Lancet 394: 882-894, 2019.
3. Rosi-Schumacher M, Baker J, Waris J, Seiffert-Sinha K and Sinha AA: Worldwide epidemiologic factors in pemphigus vulgaris and bullous pemphigoid. Front Immunol 14: 1159351, 2023.

4. Zhao W, Wang J, Zhu H and Pan M: Comparison of guidelines for management of pemphigus: A review of systemic corticosteroids, rituximab, and other immunosuppressive therapies. Clin Rev Allergy Immunol 61: 351-362, 2021.
5. Brescacin A, Baig Z, Bhinder J, Lin S, Brar L and Cirillo N: What protein kinases are crucial for acantholysis and blister formation in pemphigus vulgaris? A systematic review. J Cell Physiol 237: 2825-2837, 2022.
6. Fukaura R and Akiyama M: Targeting IL-36 in inflammatory skin diseases. BioDrugs 37: 279-293, 2023.
7. Mesas-Fernández A, Bodner E, Hilke FJ, Meier K, Ghoreschi K and Solimani F: Interleukin-21 in autoimmune and inflammatory skin diseases. Eur J Immunol 53: e2250075, 2023.
8. Liang J, Hu F, Mao L, Qiu Y, Jiang F, Wang Q, Abulikemu K, Hong Y, Ge X and Kang X: Interleukin-37 inhibits desmoglein-3 endocytosis and keratinocyte dissociation via upregulation of Caveolin-1 and inhibition of the STAT3 pathway. J Eur Acad Dermatol Venereol 37: 1920-1927, 2023.
9. Zhou J, Gemperline DC, Turner MJ, Oldach J, Molignano J, Sims JT and Stayrook KR: Transcriptomic analysis of healthy and atopic dermatitis samples reveals the role of IL-37 in human skin. Immunohorizons 5: 830-843, 2021.
10. Rønholt K, Nielsen AL, Johansen C, Vestergaard C, Fauerbye A, López-Vales R, Dinarello CA and Iversen L: IL-37 expression is downregulated in lesional psoriasis skin. Immunohorizons 4: 754-761, 2020.
11. Hou T, Tsang MS, Chu IM, Kan LL, Hon KL, Leung TF, Lam CW and Wong CK: Skewed inflammation is associated with aberrant interleukin-37 signaling pathway in atopic dermatitis. Allergy 76: 2102-2114, 2021.
12. Fujita H, Inoue Y, Seto K, Komitsu N and Aihara M: Interleukin-37 is elevated in subjects with atopic dermatitis. J Dermatol Sci 69: 173-175, 2013.
13. Gu M, Jin Y, Gao X, Xia W, Xu T and Pan S: Novel insights into IL-37: An anti-inflammatory cytokine with emerging roles in anti-cancer process. Front Immunol 14: 1278521, 2023.
14. Borgia F, Custurone P, Li Pomi F, Vaccaro M, Alessandrello C and Gangemi S: IL-33 and IL-37: A possible axis in skin and allergic diseases. Int J Mol Sci 24: 372, 2022.
15. Cavalli G and Dinarello CA: Suppression of inflammation and acquired immunity by IL-37. Immunol Rev 281: 179-190, 2018.
16. Schröder A, Lunding LP, Zissler UM, Vock C, Webering S, Ehlers JC, Orinska Z, Chaker A, Schmidt-Weber CB, Lang NJ, *et al*: IL-37 regulates allergic inflammation by counterbalancing pro-inflammatory IL-1 and IL-33. Allergy 77: 856-869, 2022.
17. Pan Y, Wen X, Hao D, Wang Y, Wang L, He G and Jiang X: The role of IL-37 in skin and connective tissue diseases. Biomed Pharmacother 122: 109705, 2020.
18. Johnston A, Gudjonsson JE, Aphale A, Guzman AM, Stoll SW and Elder JT: EGFR and IL-1 signaling synergistically promote keratinocyte antimicrobial defenses in a differentiation-dependent manner. J Invest Dermatol 131: 329-337, 2011.
19. Sayar BS, Rüegg S, Schmidt E, Sibilia M, Siffert M, Suter MM, Galichet A and Müller EJ: EGFR inhibitors erlotinib and lapatinib ameliorate epidermal blistering in pemphigus vulgaris in a non-linear, V-shaped relationship. Exp Dermatol 23: 33-38, 2014.
20. Livak KJ and Schmittgen TD: Analysis of relative gene expression data using real-time quantitative PCR and the 2(-Delta Delta C(T)) Method. Methods 25: 402-408, 2001.
21. Ramani P, Ravikumar R, Pandiar D, Monica K, Krishnan RP, Ramasubramanian A and Sukumaran G: Apoptolysis: A less understood concept in the pathogenesis of Pemphigus Vulgaris. Apoptosis 27: 322-328, 2022.
22. Hutchison DM, Hosking AM, Hong EM and Grando SA: Mitochondrial autoantibodies and the role of apoptosis in pemphigus vulgaris. Antibodies (Basel) 11: 55, 2022.
23. Sánchez-Fernández A, Zandee S, Amo-Aparicio J, Charabati M, Prat A, Garlanda C, Eisenmesser EZ, Dinarello CA and López-Vales R: IL-37 exerts therapeutic effects in experimental autoimmune encephalomyelitis through the receptor complex IL-1R5/IL-1R8. Theranostics 11: 1-13, 2021.
24. Bektas M, Jolly PS, Berkowitz P, Amagai M and Rubenstein DS: A pathophysiologic role for epidermal growth factor receptor in pemphigus acantholysis. J Biol Chem 288: 9447-9456, 2013.
25. Wang H, Peng G, Wang B, Yin H, Fang X, He F, Zhao D, Liu Q and Shi L: IL-1R(-/-) alleviates cognitive deficits through microglial M2 polarization in AD mice. Brain Res Bull 157: 10-17, 2020.
26. Schmitt T and Waschke J: Autoantibody-specific signalling in pemphigus. Front Med (Lausanne) 8: 701809, 2021.
27. Amber KT, Valdebran M and Grando SA: Non-desmoglein antibodies in patients with pemphigus vulgaris. Front Immunol 9: 1190, 2018.
28. Luo P, Feng C, Jiang C, Ren X, Gou L, Ji P and Xu J: IL-37b alleviates inflammation in the temporomandibular joint cartilage via IL-1R8 pathway. Cell Prolif 52: e12692, 2019.
29. Jia C, Zhuge Y, Zhang S, Ni C, Wang L, Wu R, Niu C, Wen Z, Rong X, Qiu H and Chu M: IL-37b alleviates endothelial cell apoptosis and inflammation in Kawasaki disease through IL-1R8 pathway. Cell Death Dis 12: 575, 2021.
30. Schumacher N and Rose-John S: ADAM17 orchestrates Interleukin-6, TNFα and EGF-R signaling in inflammation and cancer. Biochim Biophys Acta Mol Cell Res 1869: 119141, 2022.
31. Cirillo N and Prime SS: A scoping review of the role of metalloproteinases in the pathogenesis of autoimmune pemphigus and pemphigoid. Biomolecules 11: 1506, 2021.
32. Klessner JL, Desai BV, Amargo EV, Getsios S and Green KJ: EGFR and ADAMs cooperate to regulate shedding and endocytic trafficking of the desmosomal cadherin desmoglein 2. Mol Biol Cell 20: 328-337, 2009.
33. Mishra HK, Dixon KJ, Pore N, Felices M, Miller JS and Walcheck B: Activation of ADAM17 by IL-15 limits human NK Cell proliferation. Front Immunol 12: 711621, 2021.
34. Ivars M, España A, Alzuguren P, Pelacho B, Lasarte JJ and López-Zabalza MJ: The involvement of ADAM10 in acantholysis in mucocutaneous pemphigus vulgaris depends on the autoantibody profile of each patient. Br J Dermatol 182: 1194-1204, 2020.
35. Mei Y and Liu H: IL-37: An anti-inflammatory cytokine with antitumor functions. Cancer Rep (Hoboken) 2: e1151, 2019.